Translational Oncology
www.transonc.com

Volume 6 Number 2 April 2013 pp. 187–196 187

In Vitro and *In Vivo* Analysis of RTK Inhibitor Efficacy and Identification of Its Novel Targets in Glioblastomas[1,2]

Olga Martinho*,†,‡, Renato Silva-Oliveira‡, Vera Miranda-Gonçalves*,†, Carlos Clara§, José Reynaldo Almeida§, André Lopes Carvalho‡, João Taborda Barata¶ and Rui Manuel Reis*,†,‡

*Life and Health Sciences Research Institute (ICVS), Health Sciences School, University of Minho, Braga, Portugal; †ICVS/3B's, PT Government Associate Laboratory, Braga, Guimarães, Portugal; ‡Molecular Oncology Research Center, Barretos Cancer Hospital, Barretos, São Paulo, Brazil; §Department of Neurosurgery, Barretos Cancer Hospital, Barretos, São Paulo, Brazil; ¶Cancer Biology Unit, Instituto de Medicina Molecular, Faculdade de Medicina da Universidade de Lisboa, Lisboa, Portugal

Abstract

Treatment for glioblastoma consists of radiotherapy and temozolomide-based chemotherapy. However, virtually all patients recur, leading to a fatal outcome. Receptor tyrosine kinase (RTK)–targeted therapy has been the focus of attention in novel treatment options for these patients. Here, we compared the efficacy of imatinib, sunitinib, and cediranib in glioblastoma models. In the present work, the biologic effect of the drugs was screened by viability, cell cycle, apoptosis, migration, and invasion *in vitro* assays or *in vivo* by chick chorioallantoic membrane assay. Intracellular signaling was assessed by Western blot and the RTK targets were identified using phospho-RTK arrays. The amplified status of *KIT*, *PDGFRA*, and *VEGFR2* genes was assessed by quantitative polymerase chain reaction. In a panel of 10 glioblastoma cell lines, we showed that cediranib was the most potent. In addition, cediranib and sunitinib synergistically sensitize the cells to temozolomide. Cediranib efficacy was shown to associate with higher cytostatic and unique cytotoxic effects *in vitro* and both antitumoral and antiangiogenic activity *in vivo*, which could associate with its great capacity to inhibit mitogen-activated protein kinase (MAPK) and AKT pathways. The molecular status of *KIT*, *PDGFRA*, and *VEGFR2* did not predict glioblastoma cell responsiveness to any of the RTK inhibitors. Importantly, phospho-RTK arrays revealed novel targets for cediranib and sunitinib therapy. In conclusion, the novel targets found may be of value as future biomarkers for therapy response in glioblastoma and lead to the rational selection of patients for effective molecular targeted treatment.

Translational Oncology (2013) 6, 187–196

Address all correspondence to: Rui Manuel Reis, PhD, Life and Health Sciences Research Institute (ICVS), School of Health Sciences, University of Minho, Campus de Gualtar, 4710-057 Braga, Portugal. E-mail: rreis@ecsaude.uminho.pt

[1]This work was funded by Fundação para a Ciência e Tecnologia (FCT, Portugal; Project PTDC/SAU-TOX/114549/2009) and by Pfizer/Sociedade de Ciências Médicas de Lisboa with the award "Research in Oncology Diseases, Prof. Francisco Gentil." Olga Martinho is a recipient of a PhD fellowship (SFRH/BD/36463/2007), and Vera Miranda-Gonçalves is a recipient of a research fellowship (SFRH/BI/33503/2008), both from FCT. André Lopes Carvalho has a Brazilian National Council for Scientific and Technological Development Scholarship (CNPq, 313181/2009-8).
[2]This article refers to supplementary materials, which are designated by Table W1 and Figures W1 to W4 and are available online at www.transonc.com.
Received 9 November 2012; Revised 7 January 2013; Accepted 8 January 2013

DOI 10.1593/tlo.12400

Introduction

Brain tumors represent the leading cause of cancer-related death in children and the fourth in middle-aged men [1]. Gliomas are the most frequent, accounting for approximately 70% of all primary brain tumors. According to the World Health Organization, gliomas can be divided in four grades of malignancy and three histologic subtypes, being astrocytoma grade IV (glioblastoma) the most common subtype [2,3]. Glioblastomas are among the most lethal tumors, with median survival of approximately 16 months, despite aggressive surgery, radiotherapy, and chemotherapy [4]. So far, temozolomide, a cytotoxic drug, remains the only anticancer agent that has improved outcome, but almost all glioblastoma patients eventually develop tumor recurrence, resulting in death [5]. Therefore, it is imperative to improve the treatment options for glioblastoma.

Currently, there are great expectations on the translation of glioma biology [2,3] to the development of agents that target key glioma players, such as receptor tyrosine kinases (RTKs) [6]. As previously demonstrated by us and others, epidermal growth factor receptor (EGFR) alterations are the most common genetic abnormalities in malignant gliomas, alterations of 4q12 region, namely the PDGFRA, KIT, and vascular endothelial growth factor receptor 2 (VEGFR2) (KDR) amplicon, which are also frequently upregulated [7–9]. Interestingly, several recent studies showed that gliomas, and particularly glioblastomas, exhibit intratumoral heterogeneity of RTK (EGFR, PDGFRA, and MET) alterations, with individual tumors displaying co-amplification of RTKs, yet, different cells showing amplification of a different RTK [10–12]. Thus, inhibition of multiple RTKs constitutes a rational approach for treatment of these cancers. Additionally, glioblastomas are among the most human vascularized tumors, and endothelial proliferation is pathognomonic of these tumors [13]. Hence, combination of antineoplastic with antiangiogenic therapies constitutes an attractive approach [14].

Small-molecule compounds, such as imatinib, that inhibit the kinase domain of specific kinase targets have recently changed clinical practice for several advanced cancers. It has been used in the context of chronic myeloid leukemia by inhibiting the BCR-ABL fusion protein [15] and for gastrointestinal stromal tumors by inhibition of the activating KIT mutations [16]. Other drugs have been also successfully used, such as sunitinib, which inhibits VEGFR and PDGFR in metastatic renal cell carcinoma [17], and sorafenib, which targets Raf, PDGFR, VEGFR, and KIT in advanced hepatocellular carcinoma [18].

The ability of imatinib to inhibit PDGFR signaling has suggested a potential therapeutic benefit in glioblastoma. However, imatinib clinical trials showed absence or minimal therapeutic activity [19,20]. Recently, single-target bevacizumab, a humanized monoclonal antibody against VEGF, was approved by the Food and Drug Administration (FDA) for treatment of recurrent glioblastoma [21]. Although bevacizumab prolonged progression-free survival, resistance to antiangiogenic (or anti-VEGF) therapy is expected [22]. Furthermore, preclinical models suggest that anti-VEGF therapy can induce a previously noninvasive glioma tumor to invade normal brain [23]. Therefore, single-agent activity is questionable in the treatment of glioblastomas, and it is currently believed that multi-kinase inhibitors, which target several RTKs simultaneously—pan-RTK inhibitors (RTKis)—may yield greater clinical efficacy [12,24].

Sunitinib malate (SU11248, Sutent by Pfizer, New York, NY) is a small orally bioavailable molecule that has been identified as an inhibitor of the PDGFR-α/β, VEGFR1–3, KIT, RET, FLT3, and CSF1R RTKs [25]. Sunitinib has demonstrated activity in glioma preclinical mouse models [26–31] and in phase II clinical trials [32]. Cediranib (AZD2171, Recentin by AstraZeneca, London, United Kingdom) is a potent inhibitor of VEGFRs, which also targets KIT and PDGFRA [33,34]. Cediranib showed promising results in gliomas, leading to 6-month progression-free survival in phase II clinical trials [35]. The efficacy of cediranib has been related to its antiangiogenic capability and ability to normalize tumor vasculature and alleviate edema in glioma patients [36–38]. Despite the promise that the abovementioned drugs hold, the identification of biomarkers for response prediction to those therapies is a major issue that remains to be addressed.

In the present work, we first aimed to compare the therapeutic and biologic impact of three main RTKis, cediranib, sunitinib, and imatinib, in *in vitro* and *in vivo* glioblastoma models and to identify the major RTK targets in glioblastomas cells, thereby fostering the identification of potential predictive biomarkers for therapy response to these RTKis in glioblastoma.

Materials and Methods

Cell Lines and Cell Culture

Eight immortalized glioblastoma cell lines were used: SW1088, SW1783, U-87 MG, and A172 were obtained from American Type Culture Collection (ATCC, Manassas, VA), SNB-19 and GAMG were obtained from DSMZ (German Collection of Microorganisms and Cell Cultures, Braunschweig, Germany), and U251 and U373 were kindly provided by Professor Joseph Costello. All the cell lines were maintained in Dulbecco's modified Eagle's medium (DMEM 1×, high glucose; Gibco, Invitrogen, Grand Island, NY) supplemented with 10% FBS (Gibco, Invitrogen) and 1% penicillin/streptomycin solution (DMEM-10), at 37°C and 5% CO_2 [39]. Additionally, primary tumor cell cultures were derived from glioblastoma surgical biopsies obtained at the Neurosurgery Department of Barretos Cancer Hospital (São Paulo, Brazil). The study protocol was approved by the local Ethics Committee, and patients signed an informed consent form. Each tumor specimen was cut into small pieces, removing blood vessels, then resuspended in trypsin solution (Gibco, Invitrogen) and incubated at 37°C for 30 minutes. During the incubation, the suspension was pipetted up and down several times for total digestion of the tissues. The isolated cells were grown in DMEM-10. The established cell lines were characterized for the expression of glial fibrillary acidic protein (GFAP) and Nestin by immunocytochemistry (Figure W1).

Authentication of cell lines was performed by IdentiCell Laboratories [Department of Molecular Medicine (MOMA), Aarhus University Hospital Skejby, Århus, Denmark] in August 2011. Genotyping confirmed the complete identity of all cell lines, with the exception of U373, which was shown to be a subclone of the U251 cell line.

Drugs

Cediranib, sunitinib, and imatinib were obtained from Selleck Chemicals (Houston, TX) and temozolomide was obtained from Sigma-Aldrich (Sintra, Portugal). All the drugs were prepared as stock solutions in DMSO and stored at −20°C. The drugs were subsequently prepared as intermediate dilutions in DMSO to obtain an equal quantity of DMSO (1% final concentration) in each of the conditions studied. In all experimental conditions, the drugs were diluted in 0.5% FBS culture medium (DMEM-0.5) to a final concentration of 1% DMSO. Vehicle control (1% DMSO, final concentration) was also used in all experiments.

Cell Viability Assay

To determine the concentration at which 50% of the cell growth is inhibited by drug treatment (IC_{50} concentration), the cells were plated into 96-well plates at a density of 2×10^3 cells per well and allowed to adhere overnight in DMEM-10. Subsequently, the cells were treated with increasing concentrations of the drugs diluted in DMEM-0.5. After 72 hours, cell viability was quantified using CellTiter 96 Aqueous Cell Proliferation Assay (MTS) (Promega, Madison, WI). The results were expressed as mean viable cells relatively to DMSO alone (considered as 100% viability) ± SD. The IC_{50} concentration was calculated by nonlinear regression analysis using GraphPad Prism software. Combination studies with temozolomide were done using the same protocol, and the results were expressed as mean viable cells relatively to the condition of the fixed drug alone (considered as 100% viability) ± SD. Drug interactions were analyzed using CalcuSyn software. Determination of synergy was quantified by the combination index (CI).

To assess the effect of a fixed concentration of the drug in cellular viability over time, the cells were plated into 96-well plates at a density of 1×10^3 cells per well and allowed to adhere overnight in DMEM-10. Next, the viable cells were quantified using MTS assay and used as time 0 of the experience. Then, the cells were incubated with fixed concentrations of the drugs diluted in DMEM-0.5 during 24, 48, and 72 hours. At the end of each time point, cell viability was again assessed by MTS assay. The results were calibrated to the starting viability (time 0 hour, considered as 100% of viability) and expressed as the means ± SD. Both assays were done in triplicate at least three times.

Cell Cycle Analysis

The cells were plated in a six-well plate at a density of 2×10^5 cells per well and allowed to adhere overnight. After 6 hours of serum starvation, the cells were incubated for 48 hours with fixed concentrations of the drugs diluted in DMEM-0.5. Cells were trypsinized and fixed in 70% ethanol for at least 30 minutes and then stained during 1 hour at 50°C with propidium iodide (PI) solution [20 μg/ml PI and 250 μg/ml RNAse in a solution of 0.1% Triton X-100 in phosphate-buffered saline (PBS)]. Cell cycle analysis of the PI-stained cells was performed by flow cytometry (LSRII; BD Biosciences, San Jose, CA). The percentage of cells in each phase of the cell cycle was determined using FlowJo version 7.6.3, as described [39].

Wound Healing Migration Assay

The cells were seeded in six-well plates and cultured in DMEM-10 to at least 95% of confluence. Monolayer cells were washed with PBS, scraped with a plastic 200-μl pipette tip, and incubated with fixed concentrations of the drugs diluted in DMEM-0.5. The "wounded" areas were photographed by phase contrast microscopy after 0 and 48 hours. The relative migration distance was calculated by the following formula: percentage of wound closure (%) = $100(A - B)/A$, where A is the width of cell wounds before incubation, and B is the width of cell wounds after incubation [39].

Matrigel Invasion Assay

Invasion of the cells was measured using BD BioCoat Matrigel invasion chambers (BD Biosciences), as indicated by the manufacturer. Briefly, 2.5×10^4 cells were plated in the matrigel-coated 24-well transwell inserts in DMEM-0.5 containing fixed concentration of the drugs. DMEM-10 was used as chemoattractant. The cells were allowed to invade for 48 hours. The invasive cells, attached to the insert membrane, were fixed with methanol and stained with hematoxylin. The invasive cells were photographed at ×40 magnification microscope and counted in all the fields of the membrane. The results were expressed in relation to the DMSO control (considered as 100% of invasion) as the mean percentage of invasion ± SD.

Chick Chorioallantoic Membrane Assay

To assess *in vivo* tumor proliferation and angiogenesis, we used the chorioallantoic membrane (CAM) assay, as previously described [39–41]. Fertilized chicken eggs were incubated at 37°C and 70% humidity, and on day 3 of development, a window was made into the shell and the eggs were returned to the incubator. On day 9, small plastic rings were placed on the CAM. For angiogenesis assessment, 20 μl of 0.5% FBS culture medium containing fixed concentration of the drugs was injected in the ring wall over the CAM on day 14. For tumor formation evaluation, 3×10^6 cells were resuspended in 20 μl of DMEM medium and injected in the rings over the CAM on day 10. On day 14, the tumors formed were photographed *in ovo* using a stereomicroscope (Olympus S2x16). Next, 20 μl of 0.5% FBS culture medium containing 5 μM cediranib or vehicle control was injected under the tumors. At day 17 (72 hours of incubation with the drug), the tumors were again photographed *in ovo*. The chickens were sacrificed at −80°C for 10 minutes, and the tumors or CAM alone was fixed with paraformaldehyde at 4% and photographed *ex ovo*. The perimeter of the tumors was measured using Cell B software (Olympus) *in ovo* at days 14 and 17. The results were expressed as mean percentage of tumor growth for each group, from day 14 (considered as 0%) to day 17, ± SD. For blood vessel counting, photographs were taken at day 17 *ex ovo*, and the results were expressed as the mean of the vessels counted for each group of treatments ± SD.

Western Blot and Human RTK Arrays

To assess the effect of the drugs on the inhibition of intracellular signaling pathways and RTKs, the cells were cultured in DMEM-10 in T25 culture flasks, allowed to grow to 85% of confluence and then serum starved for 2 hours and incubated with the drugs, diluted in DMEM-0.5, by 2 hours. To assess apoptosis, cells were incubated with only one concentration of each drug and incubated for 12, 24, and 48 hours. At the indicated time points, the cells were washed and scraped in cold PBS and lysed in buffer containing 50 mM Tris (pH 7.6–8), 150 mM NaCl, 5 mM EDTA, 1 mM Na_3VO_4, 10 mM NaF, 10 mM sodium pyrophosphate, 1% NP-40, and 1/7 of protease cocktail inhibitors (Roche, Amadora, Portugal). Western blot analysis was done using standard 10% sodium dodecyl sulfate–polyacrylamide gel electrophoresis, loading 20 μg of protein per lane. All the antibodies were used as recommended by the manufacturer (see Supplementary Materials and Methods for antibody information). Concerning the assessment of RTK phosphorylation, a proteome Profiler human phospho-RTK antibody array (ARY001; R&D Systems, Minneapolis, MN) was used according to the manufacturer's instructions. Briefly, a total of 500 μg of fresh protein lysates was incubated overnight at 4°C with nitrocellulose membranes dotted with duplicated spots for 42 anti-RTK and control antibodies. Bound phospho-RTKs were incubated with a pan anti–phosphotyrosine-HRP antibody for 2 hours at room temperature.

Blot detection was done by chemiluminescence (ECL Western Blotting Detection Reagents, RPN2109; GE Healthcare, Piscataway, NJ) in ImageQuant LAS 4000 mini (GE Healthcare) or using X100 Hyperfilm ECL (Amersham, GE Healthcare).

Statistical Analysis

Single comparisons between the different conditions studied were done using Student's *t* test, and differences between groups were tested using two-way analysis of variance. Statistical analysis was done using GraphPad Prism version 5. The level of significance in all the statistical analyses was set at $P < .05$.

Results

Efficacy of Cediranib, Sunitinib, and Imatinib in Glioblastoma Cells

To compare the *in vitro* efficacy of cediranib, sunitinib, and imatinib treatment in glioblastomas, we determined the half-maximal inhibitory concentrations (IC_{50}) of each drug in a panel of eight glioblastoma immortalized cell lines and in two primary glioblastoma cell cultures. As shown in Table 1, cediranib was the most potent, displaying a mean IC_{50} of 1.71 ± 0.97 μM (range, 0.47–4.17 μM), whereas the mean IC_{50} for sunitinib was 2.92 ± 1.59 μM (range, 1.26–6.00 μM), and the least efficient was imatinib (mean IC_{50} of 13.01 ± 6.09 μM; range, 6.28–23.20 μM). Notably, cediranib was clearly the most potent of three RTKIs in the two primary culture glioblastoma cell lines analyzed (HCB2 and HCB7).

To evaluate the potential combinatorial value of these drugs in the context of standard glioblastoma therapy, we determined the IC_{50} of temozolomide when administrated alone or in combination with fixed doses of cediranib (1 μM to U251 and 2.5 μM to SNB-19), sunitinib (2.5 μM to U251 and 5 μM to SNB-19), and imatinib (5 μM to U251 and 15 μM to SNB-19). As exhibited in Table 2, we found that both cediranib and sunitinib synergistically sensitize glioblastoma cells to temozolomide treatment (CI < 1), whereas the effect of imatinib seems to be merely additive (CI ∼ 1).

Biologic Effect of Cediranib, Sunitinib, and Imatinib in Glioblastoma Cells

All drugs were able to reduce the viability of U251 cells over time, as assessed by MTS assay, and this effect was dose dependent (Figure 1*A*). Consistently, the effects of cediranib and sunitinib over time were the most pronounced, whereas imatinib displayed a somewhat milder inhibitory potency. To determine whether decreased viability was due to cytostatic or cytotoxic effects, we analyzed cell cycle distribution (Figure 1*B*) and poly(ADP-ribose) polymerase (PARP) cleavage (Figure 1*C*). We observed that all drugs were cytostatic, with a significant reduction of cells in S phase of the cell cycle, mainly for higher doses of treatment. Additionally, cell cycle arrest on the G_2/M phase was observed after cells were treated with 5 μM sunitinib, and a significant reduction of cells in G_0/G_1 was observed after cediranib treatment. A statistically significant higher percentage of apoptotic cells (sub-G_0) was detected only after treatment with 5 μM cediranib (Figure 1*B*). In agreement, a striking effect on PARP cleavage was detected only after high-dose cediranib treatment, whereas sunitinib and imatinib promoted only minor PARP cleavage (Figure 1*C*). Taken together, these results suggest that the high sensitivity that glioblastoma cells show to cediranib likely results from its concomitant cytostatic and cytotoxic effects.

Table 1. IC_{50} for Imatinib, Sunitinib, and Cediranib in Glioblastoma Cell Lines.

Cell Line	Mean IC_{50} ± SD (μM)*		
	Imatinib	Sunitinib	Cediranib
U251	8.3 ± 1.65	1.26 ± 0.21	1.36 ± 0.41
SNB-19	16.93 ± 0.11	6.00 ± 0.35	2.05 ± 1.34
U373	20.50 ± 0.71	3.70 ± 0.53	4.17 ± 0.75
SW1783	8.94 ± 0.76	3.23 ± 0.32	1.55 ± 0.31
U-87 MG	23.20 ± 3.11	1.38 ± 0.45	1.96 ± 0.91
GAMG	6.28 ± 0.04	1.48 ± 0.49	0.47 ± 0.35
SW1088	7.53 ± 2.16	1.68 ± 0.77	1.56 ± 0.86
A172	8.94 ± 0.23	4.87 ± 1.18	1.40 ± 0.14
HCB2	11.43 ± 0.61	3.05 ± 0.45	1.27 ± 0.29
HCB7	18.04 ± 1.75	2.59 ± 1.44	1.27 ± 0.10
Mean†	13.01 ± 6.09	2.92 ± 1.59	1.71 ± 0.97

*Mean of at least three independent experiments done in triplicate.
†Mean of the IC_{50} concentration (μM) for all cell lines.

Table 2. IC_{50} of Temozolomide in Combination with Cediranib, Sunitinib, and Imatinib.

	U251		SNB	
	TMZ IC_{50} (μM)	CI	TMZ IC_{50} (μM)	CI
TMZ alone	557.8	–	955.1	
TMZ + CD	164.0	0.838	448.7	0.985
TMZ + SU	309.4	0.837	485.0	0.866
TMZ + IM	406.2	1.176	515.4	1.033

CD, cediranib; SU, sunitinib; IM, imatinib.

Next, we addressed whether cediranib, sunitinib, or imatinib could impair cell migration and invasion *in vitro* (Figure 2). Using a wound healing migration assay, we observed that all the drugs, at higher doses, significantly inhibited cell migration and that, similar to the other assays, cediranib was the most efficient drug at the concentrations analyzed (Figure 2*A*). In contrast, only cediranib was able to impair cell invasion in a matrigel invasion assay. Surprisingly, imatinib promoted the invasion of the cells (Figure 2*B*).

The biologic effects of cediranib on viability, cell cycle, apoptosis, migration, and invasion were confirmed in another cell line (SNB-19; Figure W2). The effects of sunitinib and imatinib on viability, cell cycle, and apoptosis were comparable in both cell lines analyzed, whereas the effects on migration and invasion appeared to be cell type specific, since, in contrast to the observations in U251 cells, imatinib had no effect on cellular migration and invasion, and sunitinib efficiently inhibited invasion of SNB-19 cells (Figure W2).

To evaluate whether the antineoplastic effect of cediranib also happens *in vivo*, we induced the formation of tumors by injection of U251 cells in the CAM (Figure 3). From day 14 to day 17 of embryo development, we observed a mean growth of 69.1 ± 40.1% in the tumors treated with DMSO. In contrast, tumors treated with 5 μM cediranib showed a reduction of 59.8 ± 32.1% of the tumor growth (Figure 3*B*). Additionally, the number of blood vessels recruited to the tumors treated with cediranib was significantly reduced compared to the tumors treated with DMSO alone (mean 33.3 ± 11.9 *vs* 48.3 ± 14.2 blood vessels, respectively; $P < .05$; Figure 3*C*). Moreover, we further confirmed that all the drugs are antiangiogenic, with a significant reduction ($P < .05$) on the number of blood vessels formed after CAM treatment with 5 μM cediranib, 5 μM sunitinib, and 15 μM imatinib when compared to the drug vehicle (Figure W3).

Identification of Novel RTK Targets of Imatinib, Cediranib, and Sunitinib in Glioblastoma Cells

To characterize the molecular basis for the differential sensitivity of glioblastoma cells to the three drugs, we initially characterized the

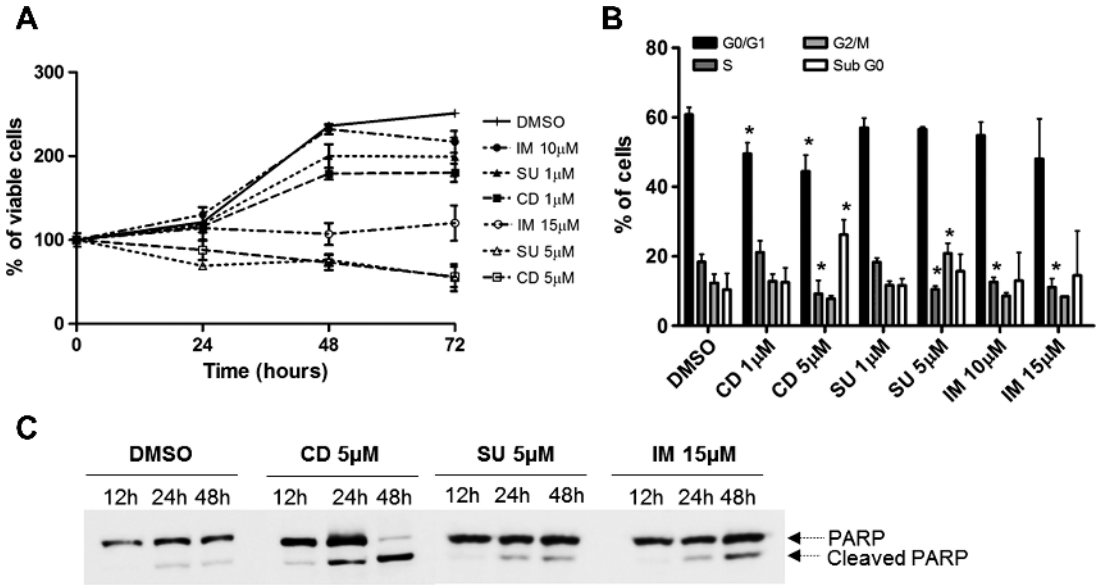

Figure 1. Effect of cediranib, sunitinib, and imatinib on U251 cellular survival, cell cycle, apoptosis, migration, and invasion. (A) Cellular viability was measured at 24, 48, and 72 hours by MTS. (B) Cell cycle analysis was done at a 48-hour time point by flow cytometric analysis of PI-stained cells. (C) Apoptosis we assessed by Western blot for PARP cleavage.

immortalized cell lines for the presence of genomic alterations of PDGFRA amplicon (4q12), in particular the *PDGFRA*, *KIT*, and *VEGFR2* genes (see Supplementary Materials and Methods). No activating mutations were found in the hotspot exons of *PDGFRA* and *KIT* oncogenes. By quantitative polymerase chain reaction (qPCR), we found co-amplification of the three genes in U251, SNB-19, and U373 cell lines. SW1783 cell line has co-amplification of *PDGFRA* and *KIT*, and GAMG cell line has amplification of

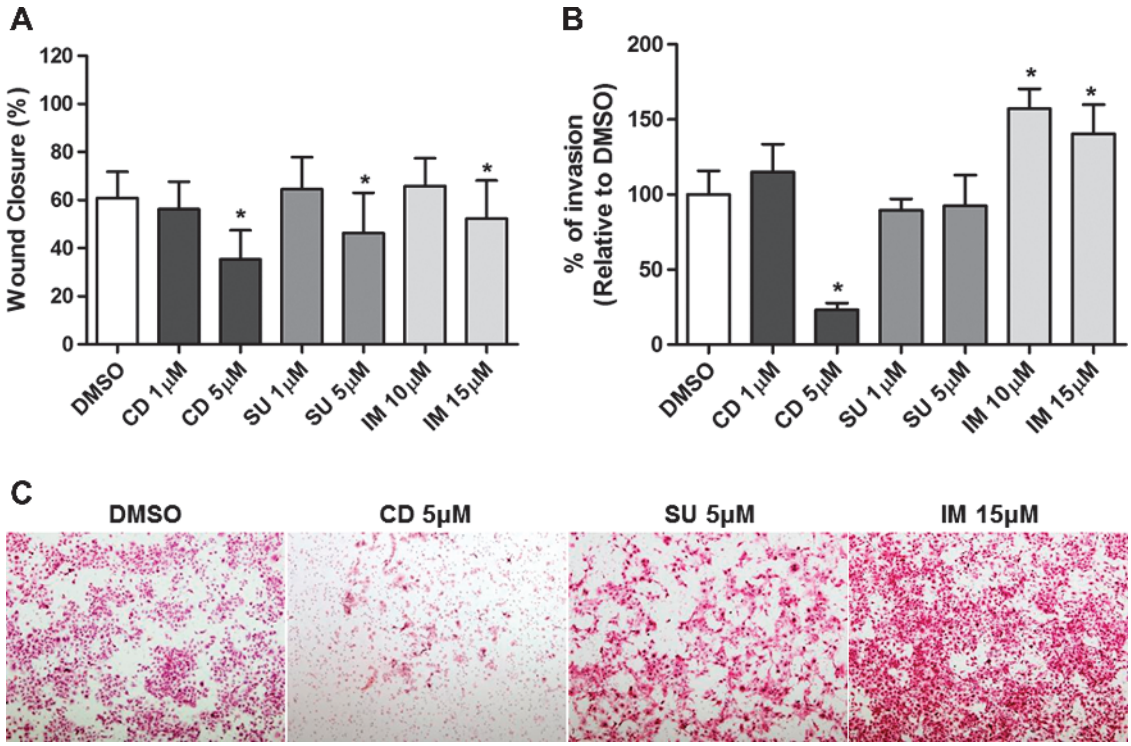

Figure 2. Effect of cediranib, sunitinib, and imatinib on U251 cellular migration and invasion. (A) Migration was measured at 48 hours by wound healing migration assay. The relative migration distance was calculated as indicated in Materials and Methods section and the results are expressed as the means ± SD. (B) Invasion was assessed by Matrigel invasion assay. The results were expressed in relation to the DMSO control (considered as 100% of invasion) as the mean percentage of invasion ± SD. (C) Representative pictures of invasion assay (×40 magnification).

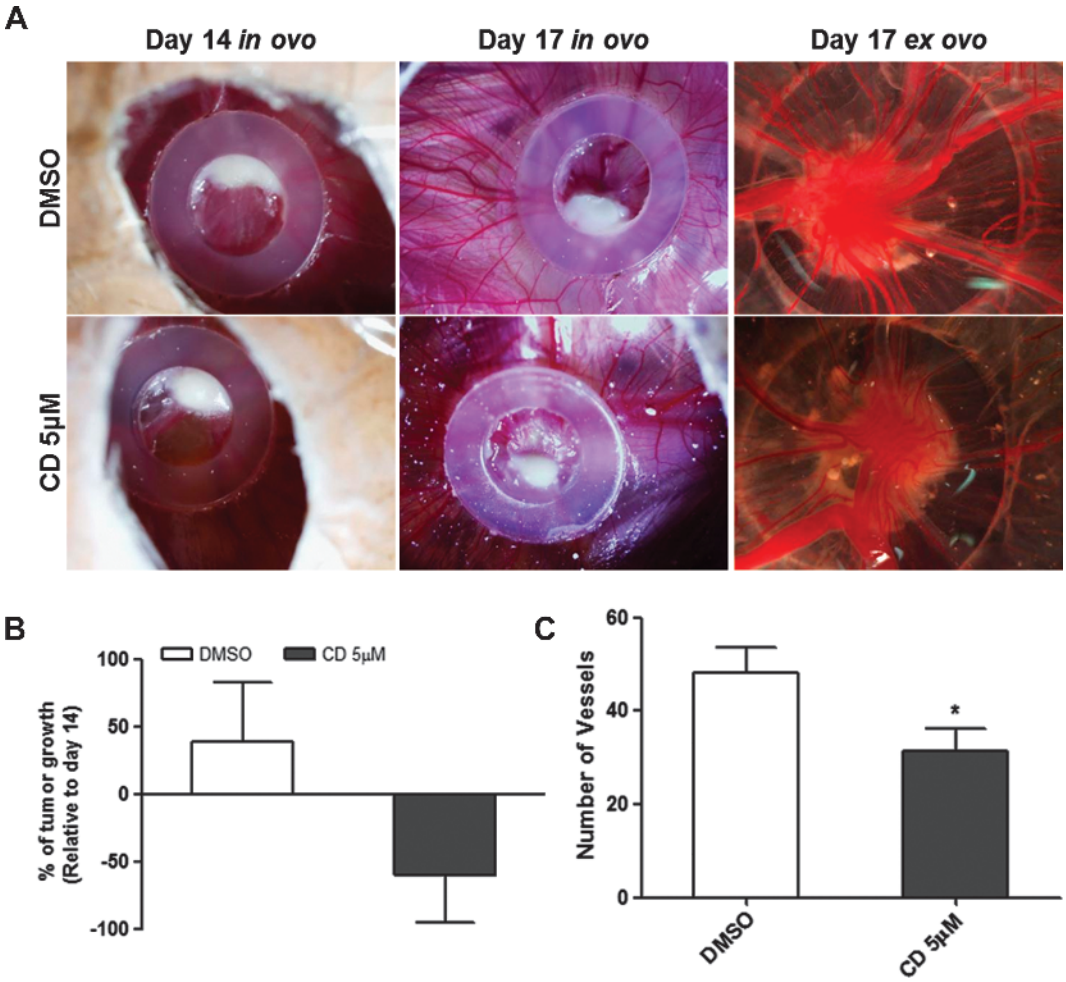

Figure 3. *In vivo* effect of cediranib on glioblastoma growth and angiogenesis. (A) Representative pictures (×16 magnification) of CAM assay *in ovo* and *ex ovo* at days 14 and 17. (B) Tumor growth was measured as described in Materials and Methods section. The results were expressed as mean percentage of tumor growth from day 14 (considered as 0%) to day 17 of development ± SD. (C) Counting of the blood vessels *ex ovo* at day 17. The results were expressed as the mean number of vessels for each group of treatments ± SD. Differences with $P < .05$ on the Student's *t* test were considered statistically significant (*). A total of 12 eggs were used for tumor formation (six were treated with cediranib and six with DMSO alone).

PDGFRA (Table W1). Subsequently, to identify the basal levels of RTK activation in the glioblastoma cell lines (including HCB7 primary cell line), we used a phospho-RTK array to assess the levels of 42 RTKs and observed that all the cell lines presented different basal levels of RTK phosphorylation (Table W1).

Next, to identify the RTKs that are targets of imatinib and mainly cediranib and sunitinib treatment in glioblastomas, we extended the RTK array analysis to some of the cell lines treated with each drug (Figures 4 and W4). As expected, we confirmed KIT and PDGFRA as common targets for both sunitinib and cediranib. Additionally, cediranib inhibited EGFR, EphA7, and AXL in all the cell lines tested that showed constitutive activation of these RTKs. MET was inhibited in the only cell line that showed basal activation of this particular RTK (GAMG cells), whereas EphB2 phosphorylation was downregulated in two of three cell lines (GAMG and HCB7). Sunitinib inhibited EphB2 in two of two cell lines (U251 and GAMG) and ROR1 in one of one (U251), whereas AXL was inhibited in SNB-19 cells but not in U251 or GAMG (Figure 4*B*). Furthermore, we observed that PDGFRA was the only target to imatinib in U251 cells (Figure 4).

In addition to RTK inhibition, we also observed activation of some RTKs after sunitinib and imatinib treatment. In U251 cells, EphB6 and Tie-1 were activated upon imatinib treatment. After sunitinib treatment, we found phosphorylation of EphA2 in U251 and GAMG cell line and also of RET in U251 cell line. We did not detect any significant increase in RTK phosphorylation after treatment with cediranib (Figures 4*A* and W4*A*).

To validate the arrays, we performed Western blot analysis for U251 cells with a specific antibody for EGFR phosphorylation (Figure W4*B*).

Effect of Cediranib, Sunitinib, and Imatinib in Intracellular Signaling Pathway Activation in Glioblastoma Cells

To further characterize the RTK inhibitors and assess whether their effects could correlate with differential activation of intracellular signaling pathways, we exposed U251 cells to increasing concentrations of the three drugs. By Western blot, we assessed the activation levels of some intermediates of the mitogen-activated protein kinase (MAPK), AKT, JAK/STAT, and SRC pathways (Figure 5). Cediranib reduced

A

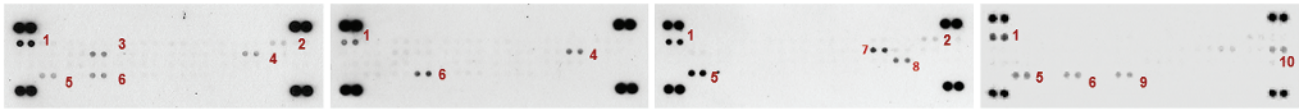

1-pEGFR; 2-pAXL; 3-pPDGFRA; 4-pROR1; 5-pEphA7; 6-pEphB2; 7-pRET; 8-pEphA2; 9-pEphB6; 10-pTie-1

B

Cell lines	Untreated	Cediranib	Sunitinib	Imatinib
U251	EGFR; EphB2; PDGFRA; ROR1; EphA7; AXL	EGFR; PDGFRA; EphA7; AXL	EphB2; PDGFRA; ROR1	PDGFRA
SNB-19	EGFR; PDGFRA; EphA7; AXL	EGFR; PDGFRA; EphA7; AXL	PDGFRA; AXL	Not done
U373	EGFR	EGFR	-	Not done
GAMG	EGFR; EphA7; FGFR3; AXL; KIT; MET; EphB2	EGFR; EphA7; AXL; KIT; MET; EphB2	KIT; EphB2	Not done
HCB7	EGFR; EphB2; Tie1; Tie2; ROR2; EphB6	EGFR	Not done	Not done

Figure 4. Cediranib, sunitinib, and imatinib targets on glioblastoma cells. (A) Representative pictures of phospho-RTK arrays for U251 cell line. Each RTK is represented in duplicate in the arrays (two spots side by side), and four pairs of phosphotyrosine positive controls are located in the corners of each array. (B) Other cell lines were treated with cediranib, sunitinib, and imatinib at the indicated concentrations, and the RTKs that were targeted after drug treatment are shown in the table.

the activation levels of extracellular signal-regulated kinase 1/2 (ERK1/2) at low doses (0.5 and 1 µM) and completely inhibited the pathway starting from 5 µM. A dose-dependent reduction of AKT activation levels was also found in cells treated with cediranib. Moreover, the activation levels of STAT3 seem to be inhibited after sunitinib and imatinib treatment.

Discussion

Molecular therapies that targeted RTKs are promising therapeutic strategies for glioblastoma tumors. However, the majority of preliminary results of clinical trials are unsatisfactory and failed to show outcome improvements, mainly because the predictive targets for therapy response in glioblastomas remain to be identified; hence, it is believed that those

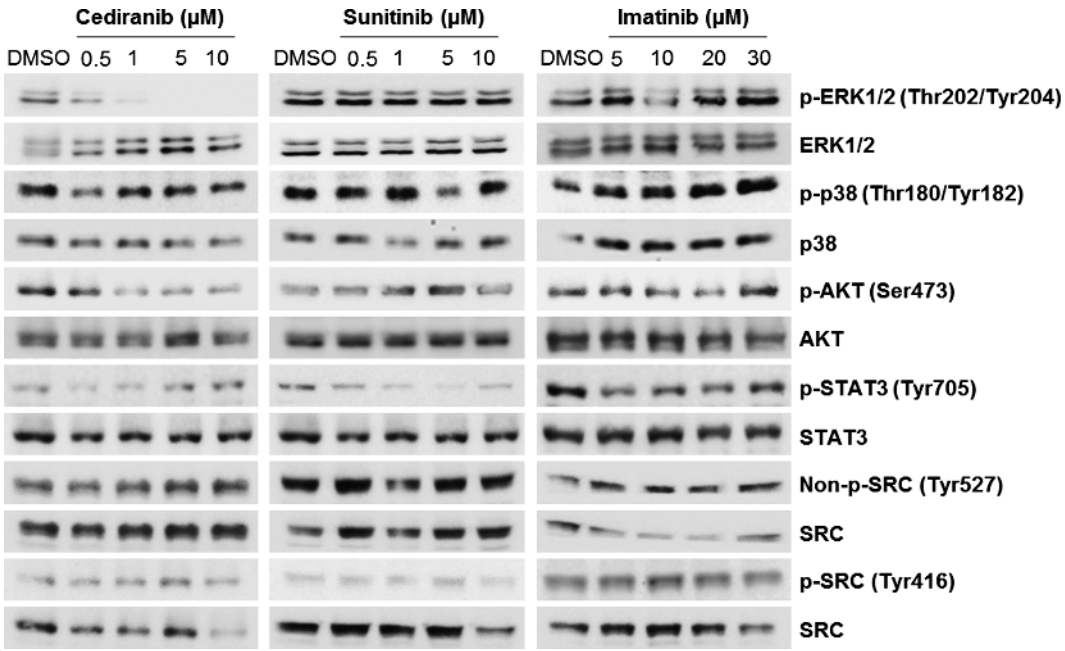

Figure 5. Effect of cediranib, sunitinib, and imatinib on intracellular signaling pathway activation in U251 cells. The cells were incubated with increasing concentrations of the three drugs by 2 hours. By Western blot, we assess the activation levels of several intermediates of the MAPK (p-ERK1/2 and p-p38), AKT (p-AKT), JAK/STAT (p-STAT3), and SRC (non-p-SRC Tyr^{527} and p-SRC Tyr^{416}) pathways. The levels of phosphorylation were compared with the corresponding total proteins.

patients are not being properly selected for the therapy [24]. In the present study, we intended to identify the specific RTK targets of two RTKis (sunitinib and cediranib). Further, we aimed to determine, *in vitro* and *in vivo*, the efficacy of these drugs in comparison to imatinib.

Hitherto, the antiproliferative effect of these drugs in glioblastomas was unclear. The reports of the effect of imatinib on glioblastoma cell proliferation impairment and cell cycle arrest are contradictory [42–45], as well as its apoptosis or autophagy consequence effect [43,44]. Concerning sunitinib, only two studies addressed its *in vitro* effects in glioblastomas, using a single cell line (U-87 MG), and found that sunitinib impairs cell survival by apoptosis induction [28,46,47] and induces cell cycle arrest in G_2/M [28]. Regarding cediranib, there are no studies reporting the effect of this drug in tumor cells *in vitro*. Two preclinical *in vivo* models showed an effect of cediranib in the reduction of xenografted tumors [48,49]. The clinical studies on glioblastoma patients showed that cediranib decreases the cell density in the central area of the tumor [50] and controls tumor growth by normalizing tumor vasculature in addition to alleviating edema [36,37]. Yet, one preclinical study with xenografted models showed that cediranib controls edema and prolongs survival but did not affect tumor growth [38].

In the present work, we found that all the drugs were effective against a panel of 10 glioblastoma cell lines (two of them being primary cultures), with cediranib being the most potent. Furthermore, we observed in U251 cells that all the drugs impair cellular survival over time and in a dose-dependent manner, and again, cediranib was the most effective, even in the less sensitive cell line (SNB-19). By cell cycle analysis, we observed that all the drugs are cytostatic and reduce the number of cells in S phase. In the cells treated with sunitinib, cell cycle arrest in G_2/M phase was also found, as described before [28]. In contrast to the other two drugs, cediranib showed to be also cytotoxic—inducing cell death by apoptosis, as assessed by PARP cleavage. We further confirmed by *in vivo* assays that cediranib displays simultaneously antiangiogenic and antitumoral activity in glioblastomas.

Glioblastomas are highly invasive tumors and this feature influences glioma survival and response to therapy [51]. Overall, we observed *in vitro* that both sunitinib and cediranib inhibited cellular migration and invasion. At variance, imatinib leads to a slight increase of both migration and invasion in some cells. There are no *in vitro* studies in the literature using cediranib in glioblastoma cells, precluding any comparisons. Concerning sunitinib, previous works on U-87 MG cells showed that sunitinib treatment was also associated with migration and invasion reduction [28,46,47]. However, invasion inhibition was not proved *in vivo* [28]. In respect to imatinib, there are only migration studies, which also reported the antimigratory capabilities of the drug in some cell lines and the absence of effect in others [52]. The effect of imatinib in glioblastoma cell invasion, as far as we know, was never reported before. Here, we observed that at least for U251 cells, imatinib can actually promote invasion. This effect was described before for other antiangiogenic drugs, such as bevacizumab [23].

The aforementioned effects are regulated by the intracellular signaling cascades. In agreement with the higher and broader activity that cediranib exhibited against glioblastoma cells, we found that cediranib inhibited both MAPK and AKT pathways, as previously described [33].

Importantly, and in agreement with other studies [48,52], we found that cediranib, as well as sunitinib, synergistically sensitizes glioma cells to temozolomide. These findings suggest that combining temozolomide with RTK inhibitor drugs may improve tumor control.

Besides the discrepant results in the preclinical models using the three drugs we tested, it has been postulated by clinical trial results that cediranib is the most promising to prolong patients' survival [32,35]. Our study, comparing the three drugs for the first time, confirmed *in vitro* the results achieved in the clinical trials, showing cediranib as the most potent antiproliferative inhibitor. However, similar to the clinical trials, we observed heterogeneous responses of the cells to the same drugs, mainly in migration and invasion assays, suggesting that each drug may have specific targets in glioblastoma cells that have yet to be identified.

The main RTK targets for the pharmacological inhibition in glioblastomas have been EGFR, PDGFRA, KIT, and VEGFR2 [6]. PDGFRA, KIT, and VEGFR2 are reported to be overexpressed, resulting from gene amplification without activating mutations [7–9]. *VEGFR2*, *PDGFRA*, and *KIT* are located side by side in the same chromosomal region 4q12, and co-amplification of these three oncogenes has been observed in glioblastoma patients [8,9]. Thus, to identify the potential targets for imatinib, sunitinib, and cediranib in glioblastomas, we first characterized the cell lines for the molecular status (mutations and amplification) of *KIT*, *PDGFRA*, and *VEGFR2*. No associations were found between the presence of those alterations and the response of the cells to the drugs. Our results are in agreement with clinical studies that failed to find associations between the presence of genomic alterations in these loci and response to sunitinib and imatinib therapy [19,32]. Next, we assessed the phosphorylation levels of 42 different RTKs, before and after treatment, using a human phospho-RTK array. We found that glioblastoma cells have coactivation of several RTKs simultaneously, as previously suggested by others [53]. Recent studies suggested that RTK amplifications (mainly EGFR and PDGFRA) in gliomas can occur in mosaic being heterogeneously distributed within single tumors [10–12]. Overall, those findings reinforce the usage of RTK multitargeted therapies, such as cediranib, for glioblastoma treatment. In the present work, we found PDGFRA as the only target of imatinib in U251 cells, and both PDGFRA and KIT were targets for cediranib and sunitinib as expected. Importantly, additional and novel targets were identified in these cells, such as EGFR, EphA7, AXL, MET, and EphB2 for cediranib and EphB2, ROR1, and AXL for sunitinib. Phyllis and colleagues showed that tumors expressing high levels of EGFR exhibited greater sensitivity to cediranib [49]. Here, we found that EGFR is one of the targets of cediranib. Overall, those findings can suggest that EGFR expression/activation can potentially be used to predict response to cediranib therapy. The role of the remaining RTK targets that we identified in glioblastoma is unclear, and their predictive value for therapy response has to be further explored.

In addition to RTK inhibition, we also observed activation of EphB6 and Tie-1 after imatinib treatment and of EphA2 and RET after sunitinib treatment. These observations, including the identification of novel targets of cediranib and sunitinib in glioblastoma and the activation of particular RTKs in some cell lines upon sunitinib and imatinib, but not cediranib, treatment, might be clinically relevant. The role of these alterations in the modulation of therapy response has yet to be determined for glioblastomas. Usually, this is a phenomenon associated with resistance of other cancers to therapy [54,55].

In conclusion, our study constitute the first comparative study of the efficacy of imatinib, sunitinib, and cediranib in glioblastoma cells and found that cediranib, either alone or in combination with temozolomide, is the most effective drug not only through its antiangiogenic activity but also as a consequence of its greater antitumoral activity. Importantly, we identified the RTK targets of cediranib and sunitinib in glioblastomas, some of which are reported for the first time.

This study constitutes a step forward in the identification of potential predictive biomarkers to anti-RTK therapies in glioblastomas that may allow, in the future, the rational selection of patients for specific targeted therapies.

References

[1] Jemal A, Bray F, Center MM, Ferlay J, Ward E, and Forman D (2011). Global cancer statistics. *CA Cancer J Clin* **61**(2), 69–90.

[2] Wen PY and Kesari S (2008). Malignant gliomas in adults. *N Engl J Med* **359**, 492–507.

[3] Huse JT and Holland EC (2010). Targeting brain cancer: advances in the molecular pathology of malignant glioma and medulloblastoma. *Nat Rev Cancer* **10**, 319–331.

[4] Niyazi M, Siefert A, Schwarz SB, Ganswindt U, Kreth FW, Tonn JC, and Belka C (2011). Therapeutic options for recurrent malignant glioma. *Radiother Oncol* **98**, 1–14.

[5] Stupp R, Hegi ME, Mason WP, van den Bent MJ, Taphoorn MJ, Janzer RC, Ludwin SK, Allgeier A, Fisher B, Belanger K, et al. (2009). Effects of radiotherapy with concomitant and adjuvant temozolomide versus radiotherapy alone on survival in glioblastoma in a randomised phase III study: 5-year analysis of the EORTC-NCIC trial. *Lancet Oncol* **10**, 459–466.

[6] Kapoor GS and O'Rourke DM (2003). Receptor tyrosine kinase signaling in gliomagenesis: pathobiology and therapeutic approaches. *Cancer Biol Ther* **2**, 330–342.

[7] Gomes AL, Reis-Filho JS, Lopes JM, Martinho O, Lambros MB, Martins A, Schmitt F, Pardal F, and Reis RM (2007). Molecular alterations of KIT oncogene in gliomas. *Cell Oncol* **29**, 399–408.

[8] Martinho O, Longatto-Filho A, Lambros MB, Martins A, Pinheiro C, Silva A, Pardal F, Amorim J, Mackay A, Milanezi F, et al. (2009). Expression, mutation and copy number analysis of platelet-derived growth factor receptor A (PDGFRA) and its ligand PDGFA in gliomas. *Br J Cancer* **101**, 973–982.

[9] Cancer Genome Atlas Research Network (2008). Comprehensive genomic characterization defines human glioblastoma genes and core pathways. *Nature* **455**, 1061–1068.

[10] Snuderl M, Fazlollahi L, Le LP, Nitta M, Zhelyazkova BH, Davidson CJ, Akhavanfard S, Cahill DP, Aldape KD, Betensky RA, et al. (2011). Mosaic amplification of multiple receptor tyrosine kinase genes in glioblastoma. *Cancer Cell* **20**(6), 810–817.

[11] Little SE, Popov S, Jury A, Bax DA, Doey L, Al-Sarraj S, Jurgensmeier JM, and Jones C (2012). Receptor tyrosine kinase genes amplified in glioblastoma exhibit a mutual exclusivity in variable proportions reflective of individual tumor heterogeneity. *Cancer Res* **72**, 1614–1620.

[12] Szerlip NJ, Pedraza A, Chakravarty D, Azim M, McGuire J, Fang Y, Ozawa T, Holland EC, Huse JT, Jhanwar S, et al. (2012). Intratumoral heterogeneity of receptor tyrosine kinases EGFR and PDGFRA amplification in glioblastoma defines subpopulations with distinct growth factor response. *Proc Natl Acad Sci USA* **109**, 3041–3046.

[13] Tuettenberg J, Friedel C, and Vajkoczy P (2006). Angiogenesis in malignant glioma—a target for antitumor therapy? *Crit Rev Oncol Hematol* **59**, 181–193.

[14] Norden AD, Drappatz J, and Wen PY (2008). Novel anti-angiogenic therapies for malignant gliomas. *Lancet Neurol* **7**, 1152–1160.

[15] Druker BJ, Sawyers CL, Kantarjian H, Resta DJ, Reese SF, Ford JM, Capdeville R, and Talpaz M (2001). Activity of a specific inhibitor of the BCR-ABL tyrosine kinase in the blast crisis of chronic myeloid leukemia and acute lymphoblastic leukemia with the Philadelphia chromosome. *N Engl J Med* **344**, 1038–1042.

[16] Demetri GD, von Mehren M, Blanke CD, Van den Abbeele AD, Eisenberg B, Roberts PJ, Heinrich MC, Tuveson DA, Singer S, Janicek M, et al. (2002). Efficacy and safety of imatinib mesylate in advanced gastrointestinal stromal tumors. *N Engl J Med* **347**, 472–480.

[17] Motzer RJ, Hutson TE, Tomczak P, Michaelson MD, Bukowski RM, Rixe O, Oudard S, Negrier S, Szczylik C, Kim ST, et al. (2007). Sunitinib versus interferon alfa in metastatic renal-cell carcinoma. *N Engl J Med* **356**, 115–124.

[18] Llovet JM, Ricci S, Mazzaferro V, Hilgard P, Gane E, Blanc JF, de Oliveira AC, Santoro A, Raoul JL, Forner A, et al. (2008). Sorafenib in advanced hepatocellular carcinoma. *N Engl J Med* **359**, 378–390.

[19] Baruchel S, Sharp JR, Bartels U, Hukin J, Odame I, Portwine C, Strother D, Fryer C, Halton J, Egorin MJ, et al. (2009). A Canadian paediatric brain tumour consortium (CPBTC) phase II molecularly targeted study of imatinib in recurrent and refractory paediatric central nervous system tumours. *Eur J Cancer* **45**, 2352–2359.

[20] Wen PY, Yung WKA, Lamborn KR, Dahia PL, Wang YF, Peng B, Abrey LE, Raizer J, Cloughesy TF, Fink K, et al. (2006). Phase I/II study of imatinib mesylate for recurrent malignant gliomas: North American Brain Tumor Consortium Study 99-08. *Clin Cancer Res* **12**, 4899–4907.

[21] Kreisl TN, Kim L, Moore K, Duic P, Royce C, Stroud I, Garren N, Mackey M, Butman JA, Camphausen K, et al. (2009). Phase II trial of single-agent bevacizumab followed by bevacizumab plus irinotecan at tumor progression in recurrent glioblastoma. *J Clin Oncol* **27**, 740–745.

[22] Wong ET, Gautam S, Malchow C, Lun M, Pan E, and Brem S (2011). Bevacizumab for recurrent glioblastoma multiforme: a meta-analysis. *J Natl Compr Canc Netw* **9**, 403–407.

[23] Keunen O, Johansson M, Oudin A, Sanzey M, Rahim SA, Fack F, Thorsen F, Taxt T, Bartos M, Jirik R, et al. (2011). Anti-VEGF treatment reduces blood supply and increases tumor cell invasion in glioblastoma. *Proc Natl Acad Sci USA* **108**, 3749–3754.

[24] De Witt Hamer PC (2010). Small molecule kinase inhibitors in glioblastoma: a systematic review of clinical studies. *Neuro Oncol* **12**, 304–316.

[25] Papaetis GS and Syrigos KN (2009). Sunitinib: a multitargeted receptor tyrosine kinase inhibitor in the era of molecular cancer therapies. *BioDrugs* **23**, 377–389.

[26] Navis AC, Hamans BC, Claes A, Heerschap A, Jeuken JW, Wesseling P, and Leenders WP (2011). Effects of targeting the VEGF and PDGF pathways in diffuse orthotopic glioma models. *J Pathol* **223**, 626–634.

[27] Chahal M, Xu Y, Lesniak D, Graham K, Famulski K, Christensen JG, Aghi M, Jacques A, Murray D, Sabri S, et al. (2010). MGMT modulates glioblastoma angiogenesis and response to the tyrosine kinase inhibitor sunitinib. *Neuro Oncol* **12**, 822–833.

[28] de Boüard S, Herlin P, Christensen JG, Lemoisson E, Gauduchon P, Raymond E, and Guillamo JS (2007). Antiangiogenic and anti-invasive effects of sunitinib on experimental human glioblastoma. *Neuro Oncol* **9**, 412–423.

[29] Zhou Q, Guo P, and Gallo JM (2008). Impact of angiogenesis inhibition by sunitinib on tumor distribution of temozolomide. *Clin Cancer Res* **14**, 1540–1549.

[30] Mendel DB, Laird AD, Xin X, Louie SG, Christensen JG, Li G, Schreck RE, Abrams TJ, Ngai TJ, Lee LB, et al. (2003). *In vivo* antitumor activity of SU11248, a novel tyrosine kinase inhibitor targeting vascular endothelial growth factor and platelet-derived growth factor receptors: determination of a pharmacokinetic/pharmacodynamic relationship. *Clin Cancer Res* **9**, 327–337.

[31] Schueneman AJ, Himmelfarb E, Geng L, Tan J, Donnelly E, Mendel D, McMahon G, and Hallahan DE (2003). SU11248 maintenance therapy prevents tumor regrowth after fractionated irradiation of murine tumor models. *Cancer Res* **63**, 4009–4016.

[32] Neyns B, Sadones J, Chaskis C, Dujardin M, Everaert H, Lv S, Duerinck J, Tynninen O, Nupponen N, Michotte A, et al. (2010). Phase II study of sunitinib malate in patients with recurrent high-grade glioma. *J Neurooncol* **103**(3), 491–501.

[33] Wedge SR, Kendrew J, Hennequin LF, Valentine PJ, Barry ST, Brave SR, Smith NR, James NH, Dukes M, Curwen JO, et al. (2005). AZD2171: a highly potent, orally bioavailable, vascular endothelial growth factor receptor-2 tyrosine kinase inhibitor for the treatment of cancer. *Cancer Res* **65**, 4389–4400.

[34] Brave SR, Ratcliffe K, Wilson Z, James NH, Ashton S, Wainwright A, Kendrew J, Dudley P, Broadbent N, Sproat G, et al. (2011). Assessing the activity of cediranib, a VEGFR-2/3 tyrosine kinase inhibitor, against VEGFR-1 and members of the structurally related PDGFR family. *Mol Cancer Ther* **10**, 861–873.

[35] Batchelor TT, Duda DG, di Tomaso E, Ancukiewicz M, Plotkin SR, Gerstner E, Eichler AF, Drappatz J, Hochberg FH, Benner T, et al. (2010). Phase II study of cediranib, an oral pan-vascular endothelial growth factor receptor tyrosine kinase inhibitor, in patients with recurrent glioblastoma. *J Clin Oncol* **28**, 2817–2823.

[36] Batchelor TT, Duda DG, Di Tomaso E, Kozak KR, Zhang W, Ancukiewicz M, Loeffler JS, Wen PY, Sorensen GA, and Jain RK (2007). Normalization of tumor vasculature and alleviation of edema by AZD2171, a pan-VEGF receptor tyrosine kinase inhibitor in glioblastoma patients. *Int J Radiat Oncol Biol Phys* **69**, S50–S51.

[37] Batchelor TT, Sorensen AG, di Tomaso E, Zhang WT, Duda DG, Cohen KS, Kozak KR, Cahill DP, Chen PJ, Zhu M, et al. (2007). AZD2171, a pan-VEGF receptor tyrosine kinase inhibitor, normalizes tumor vasculature and alleviates edema in glioblastoma patients. *Cancer Cell* **11**, 83–95.

[38] Kamoun WS, Ley CD, Farrar CT, Duyverman AM, Lahdenranta J, Lacorre DA, Batchelor TT, di Tomaso E, Duda DG, Munn LL, et al. (2009). Edema control by cediranib, a vascular endothelial growth factor receptor-targeted kinase inhibitor, prolongs survival despite persistent brain tumor growth in mice. *J Clin Oncol* **27**, 2542–2552.

[39] Martinho O, Granja S, Jaraquemada T, Caeiro C, Miranda-Goncalves V, Honavar M, Costa P, Damasceno M, Rosner MR, Lopes JM, et al. (2012). Downregulation of RKIP is associated with poor outcome and malignant progression in gliomas. *PLoS One* **7**, e30769.

[40] Silva-Correia J, Miranda-Goncalves V, Salgado AJ, Sousa N, Oliveira JM, Reis RM, and Reis RL (2012). Angiogenic potential of Gellan-gum-based hydrogels for application in nucleus pulposus regeneration: *in vivo* study. *Tissue Eng Part A* **18**(11–12), 1203–1212.

[41] Moniz S, Martinho O, Pinto F, Sousa B, Loureiro C, Oliveira MJ, Moita LF, Honavar M, Pinheiro C, Pires M, et al. (2013). Loss of WNK2 expression by promoter gene methylation occurs in adult gliomas and triggers Rac1-mediated tumour cell invasiveness. *Hum Mol Genet* **22**(1), 84–95.

[42] Hagerstrand D, Hesselager G, Achterberg S, Wickenberg BU, Kowanetz M, Kastemar M, Heldin CH, Isaksson A, Nister M, and Ostman A (2006). Characterization of an imatinib-sensitive subset of high-grade human glioma cultures. *Oncogene* **25**, 4913–4922.

[43] Shingu T, Fujiwara K, Bogler O, Akiyama Y, Moritake K, Shinojima N, Tamada Y, Yokoyama T, and Kondo S (2009). Inhibition of autophagy at a late stage enhances imatinib-induced cytotoxicity in human malignant glioma cells. *Int J Cancer* **124**, 1060–1071.

[44] Ranza E, Mazzini G, Facoetti A, and Nano R (2010). *In-vitro* effects of the tyrosine kinase inhibitor imatinib on glioblastoma cell proliferation. *J Neurooncol* **96**, 349–357.

[45] Gross D, Bernhardt G, and Buschauer A (2006). Platelet-derived growth factor receptor independent proliferation of human glioblastoma cells: selective tyrosine kinase inhibitors lack antiproliferative activity. *J Cancer Res Clin Oncol* **132**, 589–599.

[46] Dimitropoulos K, Giannopoulou E, Argyriou AA, Zolota V, Petsas T, Tsiata E, and Kalofonos HP (2010). The effects of anti-VEGFR and anti-EGFR agents on glioma cell migration through implication of growth factors with integrins. *Anticancer Res* **30**, 4987–4992.

[47] Giannopoulou E, Dimitropoulos K, Argyriou AA, Koutras AK, Dimitrakopoulos F, and Kalofonos HP (2010). An *in vitro* study, evaluating the effect of sunitinib and/or lapatinib on two glioma cell lines. *Invest New Drugs* **28**, 554–560.

[48] Wachsberger PR, Lawrence RY, Liu Y, Xia X, Andersen B, and Dicker AP (2011). Cediranib enhances control of wild type EGFR and EGFRvIII-expressing gliomas through potentiating temozolomide, but not through radiosensitization: implications for the clinic. *J Neurooncol* **105**(2), 181–190.

[49] Wachsberger PR, Lawrence YR, Liu Y, Daroczi B, Xu X, and Dicker AP (2010). Epidermal growth factor receptor expression modulates antitumor efficacy of vandetanib or cediranib combined with radiotherapy in human glioblastoma xenografts. *Int J Radiat Oncol Biol Phys* **82**(1), 483–491.

[50] di Tomaso E, Snuderl M, Kamoun WS, Duda DG, Auluck PK, Fazlollahi L, Andronesi OC, Frosch MP, Wen PY, Plotkin SR, et al. (2011). Glioblastoma recurrence after cediranib therapy in patients: lack of "rebound" revascularization as mode of escape. *Cancer Res* **71**, 19–28.

[51] Hoelzinger DB, Demuth T, and Berens ME (2007). Autocrine factors that sustain glioma invasion and paracrine biology in the brain microenvironment. *J Natl Cancer Inst* **99**, 1583–1593.

[52] Ren H, Tan X, Dong Y, Giese A, Chou TC, Rainov N, and Yang B (2009). Differential effect of imatinib and synergism of combination treatment with chemotherapeutic agents in malignant glioma cells. *Basic Clin Pharmacol Toxicol* **104**, 241–252.

[53] Stommel JM, Kimmelman AC, Ying H, Nabioullin R, Ponugoti AH, Wiedemeyer R, Stegh AH, Bradner JE, Ligon KL, Brennan C, et al. (2007). Coactivation of receptor tyrosine kinases affects the response of tumor cells to targeted therapies. *Science* **318**, 287–290.

[54] Engelman JA, Zejnullahu K, Mitsudomi T, Song Y, Hyland C, Park JO, Lindeman N, Gale CM, Zhao X, Christensen J, et al. (2007). MET amplification leads to gefitinib resistance in lung cancer by activating ERBB3 signaling. *Science* **316**, 1039–1043.

[55] Mahadevan D, Cooke L, Riley C, Swart R, Simons B, Della CK, Wisner L, Iorio M, Shakalya K, Garewal H, et al. (2007). A novel tyrosine kinase switch is a mechanism of imatinib resistance in gastrointestinal stromal tumors. *Oncogene* **26**, 3909–3919.

Supplementary Materials and Methods

Molecular Characterization of PDGFRA, KIT, *and* VEGFR2

DNA isolation was performed using TRIzol reagent (Invitrogen) as indicated by the manufacturer. The screening of mutations in the hotspot exons of *KIT* (exons 9, 11, 13, and 17) and *PDFGFRA* (exons 12, 14 and 18) was done by PCR–single-strand conformation polymorphism (SSCP), as previously described [1,2]. Assessment of *PDGFRA*, *KIT*, and *VEGFR2* gene amplification was performed by quantitative PCR, as previously described [1–3]. Primers and probes for *PDGFRA* and *KIT* amplification were previously described [1–3]. For VEGFR2, the primers and probes were the following: 5′-TGAAAGAGACACAGGAAATTACACTG-3′ (forward primer), 5′-CATAATAAATCTTGGGCAGAGAGG-3′ (reverse primer), 5′-CACAACCAGAGAGACCACATGGCTC-FL (donator probe), LC640-GCTTCTCCTTTGAAATGGGATTGGTAAGGA-3′ (acceptor probe).

Antibodies Used in the Western Blot and Array Validation

To assess the activation of intracellular signaling pathways, the antibodies used were the following: phospho-p44/42 MAPK (Thr^{202}/Tyr^{204}) (D13.14.4E); phospho-p38 MAPK (Thr^{180}/Tyr^{182}) (D3F9); phospho-Akt (Ser^{473}) (D9E); phospho-Stat3 (Tyr^{705}) (D3A7); non–phospho-Src (Tyr^{527}); phospho-Src Family (Tyr^{416}). The membranes were stripped and incubated with antibodies to detect the total protein levels as follows: p44/42 MAP kinase (137F5); p38 MAP kinase; Akt (pan) (C67E7); Stat3; Src (36D10). An antibody against PARP expression was used for apoptosis detection. When necessary, β-actin (dilution 1:300; Santa Cruz Biotechnology, Dallas, TX) was used as a loading control.

For array validation, Western blot was performed with the same lysates used for the arrays to detect EGFR phosphorylation with the specific antibody phospho-EGFR (Y1068) (D7A5) from Cell Signaling Technology (Danvers, MA). The antibody to detect total EGFR (31G7; Zymed Laboratories, San Francisco, CA) was used as controls.

Supplementary References

[1] Gomes AL, Reis-Filho JS, Lopes JM, Martinho O, Lambros MB, Martins A, Schmitt F, Pardal F, and Reis RM (2007). Molecular alterations of KIT oncogene in gliomas. *Cell Oncol* **29**, 399–408.

[2] Martinho O, Longatto-Filho A, Lambros MB, Martins A, Pinheiro C, Silva A, Pardal F, Amorim J, Mackay A, Milanezi F, et al. (2009). Expression, mutation and copy number analysis of platelet-derived growth factor receptor A (PDGFRA) and its ligand PDGFA in gliomas. *Br J Cancer* **101**, 973–982.

[3] Martinho O, Goncalves A, Moreira MA, Ribeiro LF, Queiroz GS, Schmitt FC, Reis RM, and Longatto-Filho A (2008). KIT activation in uterine cervix adenosquamous carcinomas by KIT/SCF autocrine/paracrine stimulation loops. *Gynecol Oncol* **111**, 350–355.

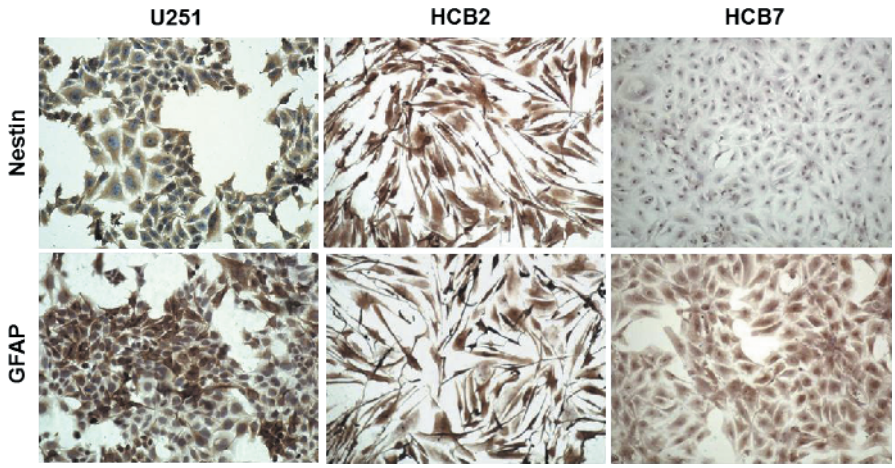

Figure W1. Immunocytochemistry analysis for Nestin and GFAP in primary cell lines (HCB2 and HCB7). U251 cell line was used as positive control. Immunocytochemistry was done with standard protocols, using specific primary antibodies for Nestin (1:200; Novus Biological, Cambridge, United Kingdom) and GFAP (1:1000; DakoCytomation, Glostrup, Denmark), followed by incubation with a biotinylated secondary antibody and revealed according to the streptavidin-biotin peroxidase complex system with visualization by 3,3′-diamonobenzidine chromogen. The pictures were taken at ×200 magnification.

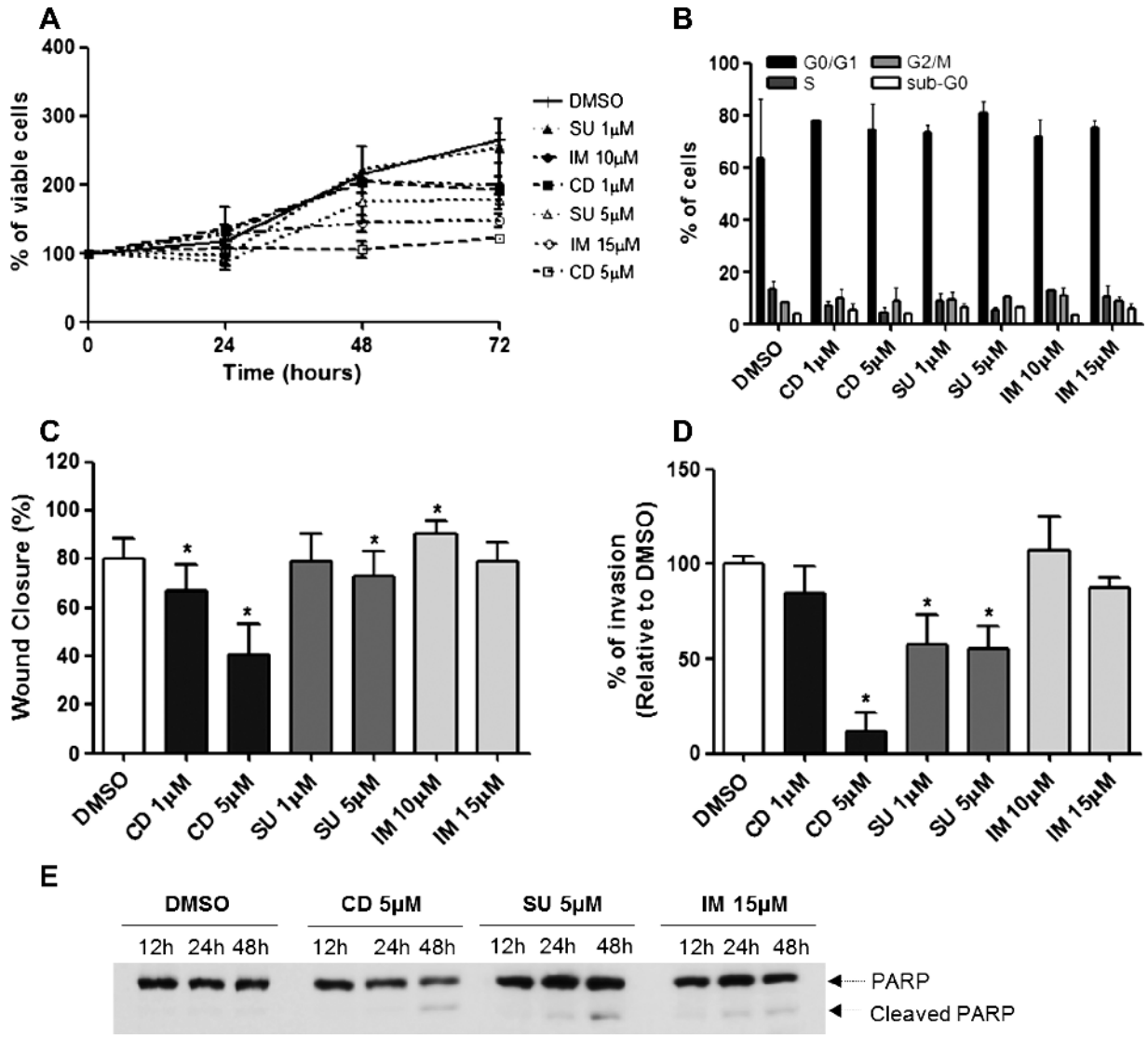

Figure W2. Effect of cediranib, sunitinib, and imatinib on SNB-19 cellular survival, cell cycle, migration, invasion, and apoptosis. (A) Cellular viability was measured at 24, 48, and 72 hours by MTS. (B) Cell cycle analysis was done at a 48-hour time point by flow cytometric analysis of PI-stained cells. (C) Migration was measured at 48 hours by wound healing migration assay. The relative migration distance was calculated as indicated in Materials and Methods section. (D) Invasion was assessed by matrigel invasion assay. (E) Apoptosis we assessed by Western blot for PARP cleavage. In all the experiments, the cells were incubated with one/two concentrations of each drug and also with the vehicle alone (DMSO) at the time points indicated. Data on A, B, C, and D are represented as the means ± SD, and differences with $P < .05$ on Student's t test were considered statistically significant (*).

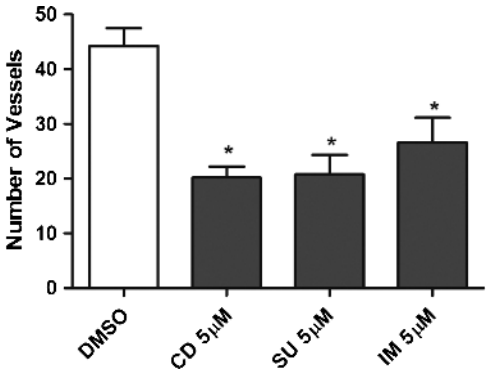

Figure W3. Effect of cediranib, sunitinib, and imatinib on angiogenesis. To assess angiogenesis, we performed CAM assay as described in Materials and Methods section. On day 14 of development, 20 μl of 0.5% FBS culture medium containing fixed concentration of the drugs (indicated in the graph) or DMSO alone was injected over the CAM. At day 17, the blood vessels were counted *ex ovo*. The results were expressed as the mean of the vessels counted for each group of treatments $\pm$ SD. Differences with $P <$ .05 on the Student's *t* test were considered statistically significant (*). A total of 20 eggs were used for angiogenesis assessment (five were treated with cediranib, five with sunitinib, five with imatinib, and five with DMSO alone).

Table W1. Molecular Alterations of RTKs in Glioblastoma Cell Lines.

Cell Line	Gene Amplification			Gene Mutations		RTK Phosphorylation*
	PDGFRA	*KIT*	*VEGFR2*	*PDGFRA*	*KIT*	
U251	Amp	Amp	Amp	wt	wt	EGFR; EphB2; PDGFRA; ROR1; EphA7; AXL
SNB-19	Amp	Amp	Amp	wt	wt	EGFR; PDGFRA; EphA7; AXL
U373	Amp	Amp	Amp	wt	wt	EGFR
SW1783	Amp	Amp	NA	wt	wt	EGFR; MSP; HER4; EphB2; PDGFRB; FGFR3; M-CSFR; ROR1
U-87 MG	NA	NA	NA	wt	wt	EGFR; MET; EphA7; MSP; HER4; EphB2; VEGFR2; FGFR3; M-CSFR; RET; ROR1
GAMG	Amp	NA	NA	wt	wt	EGFR; EphA7; FGFR3; AXL; KIT; MET; EphB2
SW1088	NA	NA	NA	wt	wt	EGFR; EphB2; PDGFRB; ROR1
A172	NA	NA	NA	wt	wt	EGFR; EphB2; PDGFRB; ROR1; AXL

Amp, amplified; NA, not amplified; wt, wild type.
*Assessed using a phospho_RTK array.

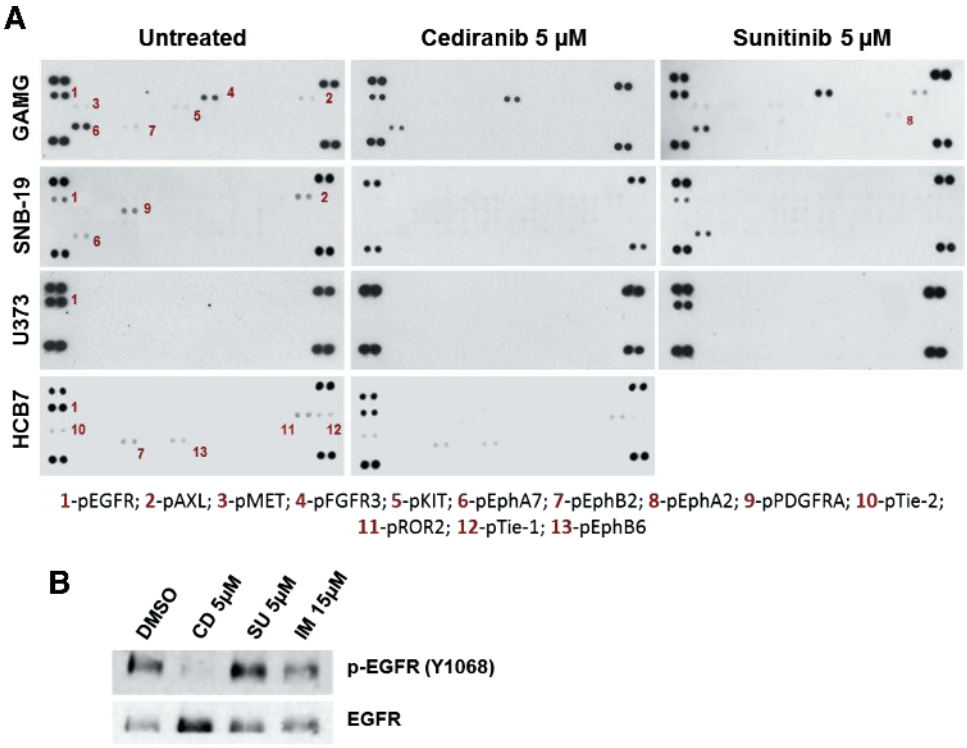

Figure W4. Cediranib and sunitinib targets in glioblastoma cells. (A) To identify the RTKs that are activated in the glioblastoma cell lines before and after cediranib and sunitinib treatment (5 μM by 2 hours), we used a phospho-RTK array (GAMG, SNB-19, U373, and HCB7 cell lines). Each RTK is represented in duplicate in the arrays (two spots side by side), and in addition, four pairs of phosphotyrosine positive controls are in the corners of each array. (B) To validate the arrays, we performed Western blot analysis with specific antibodies for EGFR phosphorylated proteins in U251 cell line treated with the three drugs.